Separation of multiphosphorylated cyclopeptides and their positional isomers by hydrophilic interaction liquid chromatography (HILIC) coupled to electrospray ionization mass spectrometry (ESI-MS)

Lana Abou Zeid, Albert Pell, Théo Tytus, Pascale Delangle, Carole Bresson

Separation of multiphosphorylated cyclopeptides and their positional isomers by hydrophilic interaction liquid chromatography (HILIC) coupled to electrospray ionization mass spectrometry (ESI-MS)

Lana ABOU ZEID[ac*], Albert PELL[a], Théo TYTUS [a], Pascale DELANGLE[b] and Carole BRESSON[a]

[a] Université Paris-Saclay, CEA, Service d'Etudes Analytiques et de Réactivité des Surfaces F-91191, Gif-sur-Yvette, France

[b] Univ. Grenoble Alpes, CEA, CNRS, IRIG, SyMMES, 38 000 Grenoble, France

[c] Sorbonne Université, UPMC, F-75005 Paris, France

*** CORRESPONDING AUTHOR:** *Lana ABOU ZEID*

Email address: lana.abouzeid@cea.fr

KEYWORDS: HILIC, hydrophilic interaction liquid chromatography, multiphosphorylated cyclopeptides, phosphopeptides isomers, retention mechanisms, ESI-MS.

Abstract

Peptides are efficient models used in different fields such as toxicology to study the interactions of several contaminants at the molecular scale, requiring the development of bio-analytical strategies. In this context, Hydrophilic interaction liquid chromatography (HILIC) coupled to electrospray ionization mass spectrometry (ESI-MS) was used to separate synthetic multiphosphorylated cyclopeptides and their positional isomers at physiological pH. We assessed (i) the selectivity of eleven HILIC columns, from different manufacturers and packed with diverse polar sorbents, and (ii) the effect of mobile phase composition on the separation selectivity. The best selectivity and baseline resolution were achieved with the columns grafted by neutral sorbents amide and diol. Furthermore, we investigated the HILIC retention mechanism of these peptides by examining the effect of the number of phosphorylated residues in the peptide scaffold on their retention. The peptide behavior followed the classical hydrophilic partitioning mechanism exclusively on amide and diol column. This trend was not fully respected on bare and hybrid silica due to the attractive/repulsive interactions of the deprotonated surface silanol groups with the Arginine or Glutamate residues in the peptide scaffold according to the peptide sequence. The position of the phosphorylated amino acid in the peptide backbone also showed to have an impact on the retention, making possible the separation of positional isomers of these multiphosphorylated cyclic peptides using HILIC.

Introduction

Peptides are efficient models to study metal-protein binding sites [1,2] and some of their derivatives have been proposed as specific metal chelators in detoxification applications [3,4] or as models of enzyme activity [5]. Peptides with sequences found in albumin [6], osteopontin [7] and calcium binding calmodulin [8] have been used to help identifying uranium (U) chelation sites in these proteins and to evaluate their affinity towards this cation, using spectroscopic techniques such as fluorescence spectroscopy, isothermal titration calorimetry (ITC), extended X-ray absorption fine structure (EXAFS) and circular dichroism. Uranyl ion displays a specific geometry that promotes coordination of ligands in the equatorial plane perpendicular to the O-U-O axis. In this context, pre-organized cyclodecapeptides designed specifically to coordinate U have been synthesized to mimic the so far unknown uranyl ion binding sites in phosphate-rich proteins, such as osteopontin [9]. In the cyclodecapeptides shown in Figure 1, the four amino acid side chains at positions 1, 3, 6, and 8 are pre-oriented in the "upper face" of the peptide scaffold to efficiently coordinate uranyl in its equatorial plane. Those amino acids were initially four glutamic acids (Glu) in pS0 [10] that were progressively replaced by phosphoserine (pSer) to obtain four pSer residues in pS1368. Peptides are named according to the number and position of the pSer residues [11–13].

In view of developing a dedicated analytical method by chromatography coupled to mass spectrometry to determine an affinity scale of these peptides towards uranium based on the separation of the uranyl-peptide complexes at physiological pH (~ 7), the prior investigation of the separation conditions and chromatographic behavior of these kind of peptides is crucial.

In the field of phosphoproteomics, various chromatographic approaches have been applied to separate phosphopeptides from their non-phosphorylated counterparts in complex samples such as proteomic digests. Dedicated methods, mainly based on multidimensional chromatography often involving ion-exchange chromatography combined with reversed-phase chromatography (RPLC) have been set up, and generally in acidic conditions [14,15]. Hydrophilic interaction liquid chromatography (HILIC) is dedicated to the separation of polar and hydrophilic molecules [16]. It combines polar stationary phases and hydro-organic mobile phases rich in organic modifier containing a volatile salt, providing

suitable conditions for ESIMS detection [17]. The analytes are retained according to their polarity and hydrophilicity through liquid-liquid partition between the mobile phase and a semi-immobilized water layer on the surface of the polar stationary phase, being the main retention mechanism [18]. Furthermore, secondary interactions such as hydrogen-bonding, dipole-dipole and electrostatic interactions generally contribute also to the retention at different degrees. Because of these features, HILIC has been more and more used these last decades to separate amino acids, peptides, metabolites and proteins [19] and has gained popularity in phosphoproteomics [20]. Using this separation mode, various polar stationary phases, mainly amide [21–24], zwitterionic [25,26], bare silica [21,22] and less frequently amino [23,27] and diol [27,28], have been used in one dimension or hyphenated with RPLC in second dimension [29,30] in studies involving unphosphorylated or multiphosphorylated linear peptides under acidic conditions. Concerning positional isomers, to our knowledge, only one study reports the separation of the positional isomers of linear multiphosphorylated peptides from protein digests, using aminopropyl HILIC stationary phase under strong acidic conditions (pH 2) [27].

The aim of this work was to set up the conditions to separate at physiological pH, synthetic pre-organized multiphosphorylated cyclodecapeptides including positional isomers (see Figure 1) using HILIC coupled to ESI-MS. In general, the peptide separations are carried out in acidic conditions but in our study, physiological pH is a key-parameter to reflect biological conditions relevant in toxicology, that are required for the following steps aiming at characterizing uranium interactions with these peptides. The selectivity of eleven polar stationary phases from different manufacturers was evaluated using different mobile phase compositions. In addition, the retention mechanisms of the peptides on the different columns were discussed, as well as the impact of the nature and the position of the amino acids in the sequence on the peptide retention.

1. Experimental part

1.1. Chemicals

Acetonitrile (ACN, CH_3CN, LC-MS grade) was supplied by VWR prolabo (Briare le canal, France). Ammonium acetate ($NH_4O_2CCH_3$) and toluene ($C_6H_5CH_3$, purity > 99.7 %) were purchased from Sigma Aldrich (Saint Quentin Fallavier, France). Ultrapure water (18.2 MΩ cm) was obtained from Milli-Q purification system (Merck millipore, Guyancourt - France).

1.2. Peptides

The peptides were synthetized, characterized using ESI-MS and circular dichroism and supplied by the CIBEST team at SyMMES (Univ. Grenoble Alpes, CEA, CNRS, IRIG, 38 000 Grenoble - France) following the procedures described elsewhere [10–13]. Table 1 summarizes nomenclature, amino acid sequence, molecular mass and the maximum charge at pH 7.4 for each peptide.

Table 1: nomenclature, amino acid sequence, molecular mass and maximum charge at pH 7.4 for each peptide.

Peptides	**Sequence** ($X_1X_2X_3X_4X_5X_6X_7X_8X_9X_{10}$)	**Molecular mass** (g mol^{-1})	**Maximum charge at pH 7.4**
pS0	c(**E**R**E**PG**E**W**E**PG)	1166.5	-3
pS1	c(**pS**R**E**PG**E**W**E**PG)	1204.5	-4
pS8	c(**E**R**E**PG**E**W**pS**PG)	1204.5	-4
pS16	c(**pS**R**E**PG**pS**W**E**PG)	1242.4	-5
pS18	c(**pS**R**E**PG**E**W**pS**PG)	1242.4	-5
pS168	c(**pS**E**E**PG**pS**W**pS**PG)	1253.3	-8
pS1368	c(**pS**E**pS**PG**pS**W**pS**PG)	1291.3	-9

X is the letter code of amino acids. pS stands for phosphorylated serine residues (pSer)

1.3. Preparation of peptide stock solutions and samples

The peptide stock solutions were prepared by dissolving the adequate amount of the targeted peptide powder in 20 mmol L^{-1} $NH_4O_2CCH_3$ (pH ~ 7) to reach a concentration between 2 and 4 mmol L^{-1}. An intermediate solution containing around 2.5 x 10^{-4} mol L^{-1} pS0, pS1/8, pS16/18 and around 5 x 10^{-4} mol L^{-1} pS168 and pS1368 was prepared by mixing the adequate volume of the peptide stock solutions

98 and adding further the appropriate volume of 20 mmol L^{-1} $NH_4O_2CCH_3$. The working samples were
99 obtained by diluting the intermediate solution in the reference mobile phase (70/30 ACN/H_2O v/v + 20
100 mmol L^{-1} $NH_4CH_4CO_2$) to reach final peptide concentrations of 5 x 10^{-5} mol L^{-1} for pS0, pS1/8 and
101 pS16/18. , and 10^{-4} mol L^{-1} pS168 and pS1368

102 ### 1.4. Instrumentation

103 Experiments were carried out using an ultimate 3000 UHPLC$^+$ Dionex/Thermofisher scientific
104 (Courtaboeuf, France), which consists of a degasser, a dual RS pump, an RS autosampler, a column
105 compartment and an RS diode array detector. A triple quadrupole TSQ Quantum Ultra^{TM} mass
106 spectrometer (Thermo Fisher scientific, San Diego CA, USA) equipped with an H-ESI II ionization
107 probe was coupled to the chromatographic system. All mass spectra were recorded in negative
108 ionization mode with the following parameters: spray voltage -3.5 kV, temperature of the probe 120
109 °C and temperature of the capillary 360 °C. Mass spectra were acquired in full scan (*m/z* 400-1500)
110 and in single ion monitoring (SIM) by selecting the *m/z* ratio associated to each peptide (spectral
111 width: ± 0.5 *m/z*).

112 ### 1.5. Chromatographic conditions

113 The peptide separations were performed with eleven columns (see Table 2) in isocratic elution.
114 Targeted mobile phase composition was obtained by online mixing of solvent A (60/40 ACN/H_2O v/v
115 + 20 mmol L^{-1} $NH_4O_2CCH_3$) and solvent B (80/20 ACN/H_2O v/v + 20 mmol L^{-1} $NH_4O_2CCH_3$) in the
116 adequate proportions. The flow rate was 300 µL min^{-1} and the injection volume was 3 µL except for
117 YMC-Triart Diol column, for which it was 1 µL.

Table 2 : Column specifications: name, manufacturer, base material, carbon load (%), surface area (m^2 g^{-1}), and column dimensions.

Stationary phase functionalization	Column name (manufacturer)	Base material	Carbon load (%)	Surface area m^2 g^{-1}
Amide	Acquity UPLC BEH amide (Waters)	Bridged ethylene hybrid BEH silica	12	185
Hybrid silica	Acquity UPLC BEH HILIC (Waters)	BEH silica	Unbonded	185
	YMC-Triart SIL (YMC)	Organic/inorganic hybrid Silica	Unbonded	330
Silica	Luna ® Silica (phenomenex)	Ultra-high purity silica	unbonded	400
Bare silica	YMC-Pack SIL (YMC)	Ultra-pure metal free silica	unbonded	330
	Hypersil GOLD™ Silica (Thermo scientific)	Highly pure base Deactivated silica	Unbonded	220
Proprietary Polar Group	Acclaim ™ HILIC-10 (Thermo scientific)	Ultrapure Silica	8	300
Diol	YMC-Triart Diol (YMC)	Organic/inorganic hybrid Silica	12	360
	Inertsil Diol (GL science)	High purity silica gel	20	450
Zwitterionic (sulfobetaine)	ZIC-pHILIC (Merck)	Polymeric	ND	ND
Amide polyol	BioZen Glycan (phenomenex)	ND	ND	200

Peptide retention factor k was calculated for each column in accordance with the following equation (1):

$$k = \frac{(t_R - t_0)}{t_0} \text{ (Equation 1)}$$

Where t_R is the retention time (min) of peptides, determined by HILIC-ESIMS, t_0 is the void time of unretained marker, toluene (10^{-4} mol L^{-1}, V_{inj} = 1 µL), determined by HILIC-UV/VIS at 254 nm.

Selectivity and resolution factors, α and R_s respectively, were calculated based on equations 2 and 3:

$$\alpha = \frac{k_2}{k_1} \text{ (Equation 2)}$$

$$R_s = 1.18 \text{ x } \frac{t_{R2} - t_{R1}}{W_{0.5h1} + W_{0.5h2}} \text{ (Equation 3)}$$

Being analyte 2 more retained than analyte 1. $W_{0.5}$ corresponds to full width half-maximum of each peak.

Asymmetry factor *As* was calculated for every separation using all the tested columns at the mobile phase composition 70/30 ACN/H_2O + 20 mmol L^{-1} $NH_4O_2CCH_3$ according to the following equation (4):

$$As = b/a \quad \text{(Equation 4)}$$

Where *a* is the width at the left half of the peak at 10% peak height and *b* is width at the right half of the peak width at 10% peak height.

2. Results and discussion

2.1. Selectivity of various polar stationary phases

The separation of peptides using the eleven columns was first assayed with a reference mobile phase consisting of ACN/H_2O 70/30 v/v + 20 mmol L^{-1} $NH_4O_2CCH_3$ [31] at physiological pH. The corresponding elution profiles (Figure 2) and the chromatographic parameters such as *k', As,* α and *Rs* (Table 3) reflect the different selectivity of the tested columns for separating the cyclopeptides in these conditions. With bioZen glycan, no elution of peptides was observed even using different mobile phase compositions. Therefore, this column is not suitable and was dropped out from the study.

Table 3: Chromatographic parameters (*k'*. *As.* α and *Rs*) calculated for the separation of the peptides with stationary phases grafted by different polar functional groups, using a mobile phase composition of 70/30 ACN/H_2O + 20 mmol L^{-1} $NH_4O_2CCH_3$.

	Amide		**Hybrid silica**						**Bare silica**				**Zwitterionic**		**Proprietary**		**Diol**			
	Acquity UPLC BEH amide		Acquity UPLC BEH HILIC		YMC-Triart SIL		Luna Silica		YMC Pack SIL		Hypersil GOLD Silica		ZIC-pHILIC		Acclaim HILIC-10		YMC Triart Diol		Inertsil Diol	
	k'	***As***	***k'***	***As***	***k'***	***As***	***k'***	***As***	***k'***	***As***	***k'***	***As***	***k'***	***As***	***k'***	***As***	***k'***	***As***	***k'***	***As***
pS0	5.7	1.0	3.2	1.0	4.7	1.3	9.3	7.8	6.6	1.4	2.7	0.8	2.4	0.7	2.1	1.5	2.8	2	1.8	1.5
pS8	7.6	1.4	4.2	5.0	6.3	1.6	19.3	/	13.2	1.6	4.4	1.5	3.0	/	2.2	/	3.3	2	2.1	/
pS1	10.4	0.8	8.4	2.4	11.8	1.7	45.8	/	31.9	1.6	12.3	1.1	3.8	/	2.6	/	4.5	2	2.5	/
pS18	12.4	2.0	9.2	/	12.9	/	ND	/	53.3	2.9	16.6		4.6	/	2.5	/	4.6	/	2.7	/
pS16	15.9	1.1	11.6	/	17.4	/	ND	/	65.7	2.0	18.8		5.4	/	3.2	/	5.9	1	3.0	/
pS168	22.4	1.7	5.4	5.3	7.3	3.7	ND	/	33.9	/	8.7	3.2	8.7	1.8	2.4	5	4.5	3	3.0	6
pS1368	27.2	2.2	7.6	3.8	9.9	6.9	ND	/	60.8	/	13.3		8.6	1.3	2.5	4.3	5.4	3	3.3	/
α	$\alpha_{pS0\text{-}pS8}$	1.3	$\alpha_{pS0\text{-}pS8}$	1.3	$\alpha_{pS0\text{-}pS8}$	1.4	$\alpha_{pS0\text{-}pS8}$	2.1	$\alpha_{pS0\text{-}pS8}$	2.0	$\alpha_{pS0\text{-}pS8}$	1.6	$\alpha_{pS0\text{-}pS8}$	1.2	$\alpha_{pS0\text{-}pS8}$	1.1	$\alpha_{pS0\text{-}pS8}$	1.2	$\alpha_{pS0\text{-}pS8}$	1.2
	$\alpha_{pS8\text{-}pS1}$	1.4	$\alpha_{pS8\text{-}pS168}$	1.3	$\alpha_{pS8\text{-}pS168}$	1.2	$\alpha_{pS8\text{-}pS1}$	2.4	$\alpha_{pS8\text{-}pS1}$	2.4	$\alpha_{pS8\text{-}pS168}$	2.0	$\alpha_{pS8\text{-}pS1}$	1.3	$\alpha_{pS8\text{-}pS168}$	1.1	$\alpha_{pS8\text{-}pS1}$	1.4	$\alpha_{pS8\text{-}pS1}$	1.2
	$\alpha_{pS1\text{-}pS18}$	1.2	$\alpha_{pS168\text{-}pS1368}$	1.4	$\alpha_{pS168\text{-}pS1368}$	1.3	ND		$\alpha_{pS1\text{-}pS168}$	1.1	$\alpha_{pS168\text{-}pS1}$	1.4	$\alpha_{pS1\text{-}pS18}$	1.2	$\alpha_{pS168\text{-}pS1368}$	1.0	$\alpha_{pS1\text{-}pS168}$	1.0	$\alpha_{pS1\text{-}pS18}$	1.1
	$\alpha_{pS18\text{-}pS16}$	1.3	$\alpha_{pS1368\text{-}pS1}$	1.1	$\alpha_{pS1368\text{-}pS1}$	1.2	ND		$\alpha_{pS168\text{-}pS18}$	1.6	$\alpha_{pS1\text{-}pS1368}$	1.1	$\alpha_{pS18\text{-}pS16}$	1.2	$\alpha_{pS1368\text{-}pS18}$	1.0	$\alpha_{pS168\text{-}pS18}$	1.0	$\alpha_{pS18\text{-}pS16}$	1.1
	$\alpha_{pS16\text{-}pS168}$	1.4	$\alpha_{pS1\text{-}pS18}$	1.1	$\alpha_{pS1\text{-}pS18}$	1.1	ND		$\alpha_{pS18\text{-}pS1368}$	1.1	$\alpha_{pS1368\text{-}pS18}$	1.3	$\alpha_{pS16\text{-}pS1368}$	1.6	$\alpha_{pS18\text{-}pS1}$	1.1	$\alpha_{pS18\text{-}pS1368}$	1.2	$\alpha_{pS16\text{-}pS168}$	1.0
	$\alpha_{pS168\text{-}pS1368}$	1.2	$\alpha_{pS18\text{-}pS16}$	1.3	$\alpha_{pS18\text{-}pS16}$	1.4	ND		$\alpha_{pS1368\text{-}pS16}$	1.1	$\alpha_{pS18\text{-}pS16}$	1.1	$\alpha_{pS1368\text{-}pS168}$	1.0	$\alpha_{pS1\text{-}pS16}$	1.2	$\alpha_{pS1368\text{-}pS16}$	1.1	$\alpha_{pS168\text{-}pS1368}$	1.1
Rs	$Rs_{pS0\text{-}pS8}$	1.7	$Rs_{pS0\text{-}pS8}$	1.5	$Rs_{pS0\text{-}pS8}$	1.4	$Rs_{pS0\text{-}pS8}$	2.3	$Rs_{pS0\text{-}pS8}$	4.1	$Rs_{pS0\text{-}pS8}$	2.3	$Rs_{pS0\text{-}pS8}$	1.1	$Rs_{pS0\text{-}pS8}$	0.6	$Rs_{pS0\text{-}pS8}$	0.9	$Rs_{pS0\text{-}pS8}$	0.7
	$Rs_{pS8\text{-}pS1}$	2.2	$Rs_{pS8\text{-}pS168}$	1.0	$Rs_{pS8\text{-}pS168}$	0.5	$Rs_{pS8\text{-}pS1}$	3.0	$Rs_{pS8\text{-}pS1}$	6.5	$Rs_{pS8\text{-}pS168}$	3.5	$Rs_{pS8\text{-}pS1}$	1.4	$Rs_{pS8\text{-}pS168}$	0.5	$Rs_{pS8\text{-}pS1}$	2.4	$Rs_{pS8\text{-}pS1}$	1.1
	$Rs_{pS1\text{-}pS18}$	1.2	$Rs_{pS168\text{-}pS1368}$	0.5	$Rs_{pS168\text{-}pS1368}$	0.9	ND		$Rs_{pS1\text{-}pS168}$	0.4	$Rs_{pS168\text{-}pS1}$	2.2	$Rs_{pS1\text{-}pS18}$	1.1	$Rs_{pS168\text{-}pS1368}$	0.2	$Rs_{pS1\text{-}pS168}$	0.0	$Rs_{pS1\text{-}pS18}$	0.4
	$Rs_{pS18\text{-}pS16}$	1.8	$Rs_{pS1368\text{-}pS1}$	0.2	$Rs_{pS1368\text{-}pS1}$	0.7	ND		$Rs_{pS168\text{-}pS18}$	2.9	$Rs_{pS1\text{-}pS1368}$	0.4	$Rs_{pS18\text{-}pS16}$	1.0	$Rs_{pS1368\text{-}pS18}$	0.0	$Rs_{pS168\text{-}pS18}$	0.2	$Rs_{pS18\text{-}pS16}$	0.5
	$Rs_{pS16\text{-}pS168}$	2.8	$Rs_{pS1\text{-}pS18}$	0.6	$Rs_{pS1\text{-}pS18}$	0.4	ND		$Rs_{pS18\text{-}pS1368}$	0.7	$Rs_{pS1368\text{-}pS18}$	1.4	$Rs_{pS16\text{-}pS1368}$	2.8	$Rs_{pS18\text{-}pS1}$	0.4	$Rs_{pS18\text{-}pS1368}$	1.0	$Rs_{pS16\text{-}pS168}$	0.0
	$Rs_{pS168\text{-}pS1368}$	1.6	$Rs_{pS18\text{-}pS16}$	1.0	$Rs_{pS18\text{-}pS16}$	1.1	ND		$Rs_{pS1368\text{-}pS16}$	0.4	$Rs_{pS18\text{-}pS16}$	0.9	$Rs_{pS1368\text{-}pS168}$	0.1	$Rs_{pS1\text{-}pS16}$	1.0	$Rs_{pS1368\text{-}pS16}$	0.6	$Rs_{pS168\text{-}pS1368}$	0.4

ND: Not Detected; /: *As* cannot be calculated due to (i) unresolved peaks or (ii) 10 % of the peak height < baseline noise.

Bare silica columns such as Luna Silica. YMC-Pack SIL and Hypersil GOLD Silica display a highly polar and negatively charged stationary phase at pH 7 due to deprotonated surface silanol groups. Because of this high polarity, the highest retention factors of all the peptides were obtained with the first two columns among all the tested ones with *k'* reaching for example 45.8 and 31.9 for monophosphorylated pS1 on Luna Silica and YMC-Pack SIL (see Table 3). It must be noticed that retention is significantly lower for the Hypersil GOLD Silica, with k'=12.3 for pS1. The retention of the negatively charged peptides displaying the same charge as the stationary phase reflects that the main retention mechanism-taking place is hydrophilic partitioning with respect to electrostatic repulsions, that solely would lead to decreased or no retention of analytes. The retention of analytes displaying the same charge as the stationary phase is one of the HILIC features compared to ion exchange chromatography [32].

In the case of the highly retentive Luna Silica, only broad peaks were observed for pS0, pS1 and pS8, while none of the remaining multiphosphorylated peptides was observed using this mobile phase composition. In the same conditions, all the peptides were eluted with the YMC-Pack SIL and Hypersil GOLD Silica columns. This difference is attributed to the surface area of the columns, varying as follows: Hypersil GOLD Silica < YMC-Pack SIL < Luna Silica (Table 2) and leading to increasing retention of peptides accordingly. Using YMC-Pack SIL and Hypersil GOLD Silica, pS16 was the most retained peptide with *k'* = 65.7 and 18.8, respectively. Overall, a good separation of the pS8-pS1 positional isomers was achieved with the three columns with selectivity factors of 2.4 for Luna Silica and YMC-Pack SIL and 2.8 for Hypersil Gold Silica.

Hybrid silica Acquity UPLC BEH HILIC and YMC-Triart SIL columns contain non-grafted stationary phases, made of supports with different hybrid technologies. Bridged ethylene hybrid (BEH) supports consist of ethylene bridges embedded within the silica matrix that coat nearly one-third of the surface silanols [33]. YMC-Tiart SIL is based on hybrid particles with multi-layered organic/inorganic silica [34]. Hybrid supports provide stationary phases with lower deprotonated surface silanol groups and decreased polarity compared to bare silica columns, leading to lower peptide retention factors as can be seen in Figure 2 and Table 3. For example, pS1 retention factor is three times lower with YMC-Triart SIL (*k'* = 11.8) than with YMC-Pack SIL (*k'* = 31.9). As observed with bare silica columns, the

peptides were more retained on the column exhibiting the higher surface area that is the YMC-Triart SIL with respect to the Acquity UPLC BEH HILIC (Table 2) and pS16 was eluted with the highest retention factor with both hybrid silica columns.

The remaining columns are based on bare or hybrid silica supports, grafted with different functional groups such as amide, diol and zwitterionic.

Acquity UPLC BEH amide is based on hybrid silica support, grafted with neutral amide groups through an alkyl spacer. As neutral stationary phase, analyte retention is driven by hydrophilic partitioning as main mechanism and hydrogen bonding also contribute to the retention owing to the hydrogen donor and acceptor ability of the amide group. Accordingly, the retention factors of the peptides increased with respect to the number of pSer residues in the peptides scaffold in agreement with their increasing polarity and hydrophilicity (Figure 2 and Table 3). Amide stationary phase displayed high separation selectivity and baseline resolution for separating these cyclic peptides, including their positional isomers ($Rs_{\text{pS8-pS1}} = 2.2$ and $Rs_{\text{pS18-pS16}} = 1.8$).

Acclaim HILIC-10 is based on bare silica support, grafted with a proprietary hydrophilic functional group. It showed weak retention of the peptides leading to co-elution of most of them and a poor baseline resolution ($Rs < 1.5$ as shown in Table 3). This reflects the insufficient polarity of the functional group for separating these peptides under the selected conditions.

ZIC-pHILIC is a zwitterionic column, made of a polymer material grafted with a sufoalkylbetaine chain that contains both negatively charged sulfonic acid and positively charged quaternary ammonium separated by a short alkyl spacer. As the two oppositely charged groups are present in equimolar ratio, the zwitterionic function is globally neutral. Sulfoalkylbetaine columns strongly adsorb water, therefore hydrophilic partitioning is the main retention mechanism of the analytes. but weak electrostatic interactions contribute to the retention of charged analytes as well as hydrogen bonding [17]. Taking into account these features, the retention of the peptides increased in connection with the number of pSer groups, even though in this mobile phase composition peaks are poorly resolved ($Rs < 1.5$. except for pS16-pS1368 $Rs = 2.8$. see Table 3) and the tri- and tetraphosphorylated peptides were co-eluted (Figure 2).

YMC-Triart Diol and Inertsil Diol columns are respectively based on hybrid and pure silica supports, grafted with neutral dihydroxypropyl groups through a spacer. The separation is based on hydrophilic partioning as major retention mechanism, in combination with hydrogen bond interactions through the OH group. Using the reference mobile phase, the peptides were weakly retained and almost co-eluted, which is explained by the low polarity and hydrophilicity of diol stationary phases. The retention factors are slightly different with both columns despite being grafted with the same functional group. For example k'_{pS1} with YMC-Triart Diol (k' = 4.5) is almost twice the observed with Inertsil Diol (k' = 2.5). It is important to mention that despite having a hydroxy group on both diol columns, they display differences in the carbon chain length, which is higher for Inertsil Diol. In addition, this latter has an ether group in its chain, which is not present with YMC-Triart Diol (see Table 2). This illustrates that columns categorized as same stationary phase are different between manufacturers in the architecture of the functional group, the grafting rates and the technology of the material support.

The first screening of various columns for separating multiphosphorylated cyclic peptides using a fixed mobile phase composition showed diverse selectivity according to the chemical group bonded to the stationary phase. Acquity UPLC BEH amide showed to be suitable for the separation of the peptides. These latter displayed a different chromatographic behavior with the remaining columns and in some cases, we obtained a good separation of the positional isomers, making interesting a further investigation of the effect of mobile phase composition on the separation selectivity mechanism of these phosphorylated cyclopeptides and of their HILIC retention mechanism.

2.2. Effect of mobile phase composition

The mobile phase's elution force is another parameter influencing the separation selectivity in HILIC and is highly related to organic content of the mobile phase. By way of example. Figure 3 shows the chromatographic behavior (Figure 3A) and the retention factors of the peptides (Figure 3B) in function of the mobile phase's organic content for columns of increasing polarity: Acclaim HILIC-10, diol (YMC-Triart Diol). Zwitterionic (ZIC-pHILIC) and bare silica (YMC-Pack SIL). In all cases, the salt concentration was kept at 20 mmol L^{-1}.

As previously observed, 70% ACN in the mobile phase induced unacceptable retention factors with the more polar bare silica columns. We therefore assessed the effect of higher mobile phase's elution

231 force for this class of stationary phases by decreasing the proportion of ACN. This latter was
232 decreased up to 40 % with the highly retentive Luna Silica column, but pS168 and pS1368 were still
233 not eluted and pS18 and pS16 were eluted near the void time (data not shown), rendering this column
234 not suitable for the rest of the study. For YMC-Pack SIL, the peptide retention factors of all the
235 peptides decreased with the ACN percentage as expected (Figure 3A and B). It must however be
236 noticed that elution order changed between pS168 and pS1368 and their neighboring peptides when
237 the mobile phase's elution force was modified (Figure 3B). The same behavior was observed on
238 Hypersil Gold Silica but only for pS1368 (see Table 3 and Supporting Information).
239 For the less polar remaining columns, the elution force was decreased by increasing the mobile phase
240 organic content, promoting the retention of the peptides in all cases. With the Acclaim HILIC-10, the
241 ACN content was increased up to 77%, but the selectivity was still insufficient (Figure 3A) and the
242 separation of the peptides was not achieved. A composition of 80 % ACN did not improve the
243 separation performance either and yielded retention factors up to 28.5 with very wide peaks.
244 Concerning the YMC-Triart Diol, the ACN content was increased up to 75 % giving a good separation
245 selectivity ($1.1 < \alpha < 1.5$) and baseline resolution ($Rs > 1.5$) except for the pS168/pS16 ($Rs_{pS168\text{-}pS16}$ =
246 0.9) and pS1/pS18 ($Rs_{pS1\text{-}pS18} = 1.4$) pairs (See Supporting Information). A change in the elution order
247 was also observed between pS168 and pS1368 and their neighboring peptides at 72% and 74% ACN
248 respectively (Figure 3A and B). We could suggest that a change in the retention mechanism occurred
249 and that secondary interactions of the peptides with the stationary phase through hydrogen bonding
250 took more important part. For Inertsil Diol, increasing the ACN content up to 75% improved the
251 separation selectivity but was still insufficient due to the wide peaks obtained at this percentage (see
252 Supporting Information). Contrary to YMC-Triart Diol, we observed no change in the elution order of
253 the peptides while modifying the mobile phase composition. For ZIC-pHILIC column, the peptides
254 were eluted in two groups whatever the ACN content. The first one includes peptides with 0, 1 and 2
255 pSer residues and their positional isomers, which were separated with a good selectivity and baseline
256 resolution at 72% ACN ($1.5 < Rs < 2$ .4 and $\alpha > 1$). The second one includes tri- and
257 tetraphosphorylated peptides pS168 and pS1368, which were co-eluted at all the mobile phase
258 compositions. It must be noticed that pS1368 displayed a very large peak at 74% and 76% ACN,

making difficult the precise identification of the apex. With hybrid silica columns (see Table 1), the ACN amount was increased up to 74 % which did not improve the separation performance and lead to very large peaks and co-elution of some of the peptides (data not shown).

Overall, the mobile phase modification induced in some cases an inversion of the elution order only between the tri- and tetra- phosphorylated peptides pS168 and pS1368 and their neighboring peptides respectively. This result reflects that pS168 and pS1368 are more sensitive to the mobile phase polarity than the other peptides.

2.3. HILIC behavior of the multiphosphorylated cyclopeptides

It is commonly known that in HILIC. retention increases with analyte polarity [17]. Therefore, higher retention of the peptides is expected by increasing the number of polar pSer residues in their scaffold. As previously shown, this was not always the case in our study and we rather observed two trends in the elution order of the peptides depending on the stationary phase grafting.

In order to illustrate the effect of phosphate groups (pSer) on the retention of the cyclic peptides, their retention factors *k'* were plotted against the number of pSer in the sequence. In each case, the mobile phase composition was chosen to obtain *k'* less than 30, while keeping satisfying resolution and selectivity (see Figure 4).

A linear correlation between the retention factor and the number of pSer was observed exclusively using the neutral amide-grafted (R^2 = 0.9489) and Inertsil Diol-grafted (R^2 = 0.9315) columns. The peptide hydrophilicity increases with the number of negatively charged pSer residues, inducing higher retention, in agreement with classical HILIC behavior. Our results are similar to those obtained by Singer *et al.*. who separated multiphosphorylated linear peptides with 0. 1. 2 and 3 phosphorylation sites using a diol column. leading to increased retention in accordance with the number of phosphorylation residues [27]. Furthermore, Yanagida *et al.* obtained also high correlation between logk and the increasing number of hydroxy groups (-OH) in proanthocyanidins, using a TSKgel Amide-80 column, and showed that it was the result of the dominance of secondary interactions through hydrogen bonding on hydrophilic partitioning mechanism [35].

When using stationary phases involving electrostatic interactions, the peptides behave differently (Figure 4). With the bare and hybrid silica columns, the retention factors increased with the number of pSer residues for pS0, pS1-pS8, pS18-pS16 (group A) and then decreased for pS168 and pS1368 (group B).

All of the peptides display a global negative charge because of the presence of negatively charged amino acids such as Glu (pKa = 4.07) and/or pSer (pKa_1 = 2.1 pKa_2 = 5.8), at position 1. 3. 6 and 8. Their backbone is made of neutral amino acids Pro. Gly at position 4. 5. 9. 10 and Trp at position 7, but the amino acid at position 2 is Arg (pKa = 12.10. charge +1) for the group A and Glu (pKa = 4.07. charge -1) for the group B. This difference affects the global negative charge of the peptides, for which the maximum charge at pH 7 increases as follows: pS0 (-3), pS8/1 (-4), pS18/16 (-5), pS168 (-8) and pS1368 (-9). It is important to mention that the amino acids located in position 2 (Arg) and 7 (Trp) are orientated in the "lower face" of the peptide scaffold, contrary to the ones in position 1. 3. 6 and 8, that might affect their retention, since different group of different charge is available towards the surface of the stationary phase.

Since bare and hybrid silica columns display free negatively charged deprotonated silanol groups on their surface, electrostatic interactions contribute also to the retention of the peptides in addition to hydrophilic partitioning. Concerning the group A peptides, additional attractive electrostatic interactions taking place between the negatively charged silanol groups of the stationary phase and the Arg seem to promote their retention. We can assign this behavior to the one described by Alpert as the "contact region of peptides" in HILIC. being the region of these latter that preferentially interact with the stationary phase [36]. Gilar and Jaworski, who studied the HILIC behavior of tryptic linear peptides at pH 4.5 using bare, hybrid, and amide columns have discussed the Arg impact on the peptide retention [21]. Their experiments, along with their retention prediction models, showed that positively charged Arg residues strongly promoted the peptide retention on columns exhibiting deprotonated negatively charged surface silanols such as bare and hybrid silica *via* cation exchange interactions. This trend was more significant with bare silica compared to hybrid silica columns, due to the differences in deprotonated silanol amount on the surface, which is in agreement with our results [21].

Figure 4 shows that pS168 and pS1368 had lower retention factors compared to group A peptides. These two peptides bear only negatively charged amino acids and the highest negative charge among the peptides, leading to electrostatic repulsions with the stationary phase and therefore reduced retention. This might explain why the retention factors of these peptides were highly affected by the slightest change of mobile phase composition compared to other peptides.

This different behavior between group A and group B peptides is surprisingly observed with some neutral columns such as YMC-Triart Diol and Acclaim-HILIC-10, but is less pronounced. This means that residual deprotonated surface silanols are more accessible on these columns to interact with the analytes and thus influence their retention factors despite being shielded by neutral functionalization. Finally, the ZIC-pHILIC column showed similar behavior for group A peptides whilst pS168 and pS1368 of group B are co-eluted. However, these latter are more retained than the first group, meaning that the nature and the charge of the amino acid in position 2 did not affect the retention. The secondary weak electrostatic interactions combined with the hydrophilic partitioning did not provide enough selectivity to separate these two peptides. This was the case at all mobile phase compositions, as seen in the previous part.

The HILIC behavior of the multiphosphorylated cyclic peptides differed in connection with the charged amino acids (Arg and Glu) in the lower face of the peptide backbone on all the tested columns, except for the amide and inertsil diol for which residual deprotonated silanols had negligible effect.

2.4. Impact of amino acid position on the HILIC retention of the peptides

The positional isomers of mono- and di-phosphorylated peptides differ only by the location of one pSer residue in the sequence, as can be seen in pS1 c(**pS**REPGEWEPG)/pS8 c(EREPGE**W**p**S**PG) and pS16 c(**pS**REPG**pS**WEPG)/pS18 c(**pS**REPGE**W**p**S**PG) (Figure 1). We achieved a successful separation of these positional isomers with most of the columns, leading to systematic stronger retention of pS1 and pS16 compared to pS8 and pS18 respectively. This shows that the position of the pSer residue significantly affect the HILIC behavior of the peptides. In the mono- and di-phosphorylated peptides, the pSer residue in position 8 is neighbored by Pro and Trp amino acids, while in their positional isomers it lies between Gly and Arg for pS1 and Gly and Trp for pS16 (Figure

341 1). Moreover, in pS16, both pSer residues are located close to Gly residues. We can suggest that the
342 Pro and Trp amino acids close to pSer induce higher steric hindrance in pS8 and pS18 than the amino
343 acids in their isomer counterparts, making thus the pSer residue less available to interact with the
344 stationary phase and therefore lower retention of pS8 and pS18 than pS1 and pS16.
345 The major effect of amino acid position in the peptide sequence on retention in HILIC has also been
346 reported in the literature based on prediction models and experimental investigations [21.24.28] using
347 linear peptides, where amino acid were positioned at N-terminus or at different other positions.
348 Although peptides involved in our work are cyclic and structured, we obtained results in agreement
349 with these studies.

Conclusion

The main objective of this work was to separate synthetic multiphosphorylated cyclopeptides and their positional isomers at physiological pH using HILIC coupled to ESI-MS. and to shed light on their retention mechanisms. By screening several stationary phases and mobile phase compositions, the best separation selectivity and baseline resolution were achieved by using columns grafted with neutral amide (Acquity UPLC BEH amide) and diol (YMC-Triart Diol) functional groups, with a mobile phase containing 70 and 75 % ACN and 20 mmol L^{-1} ammonium acetate, respectively (see Figure 2 and Figure 3A).

The HILIC retention mechanism study showed that peptide retention factors followed the classical HILIC mechanism with the amide and Inertsil Diol-grafted columns, and a linear correlation between retention factors and the number of polar phosphorylated residues was obtained. With the remaining columns, we observed that the nature and charge of the amino acid at the lower face of the peptide backbone affected the peptide retention, depending on the contribution part of the secondary electrostatic interactions with the residual deprotonated silanols at the surface of the stationary phase. The position of the amino acid in the backbone had also an impact on the peptide retention, making it possible the separation of mono- and di-phosphorylated positional isomers with satisfying baseline resolution. The next step of this work will focus on the separation of uranium complexes formed with these peptides at physiological pH and the quantification of uranium among these peptides, using HILIC coupled to elemental and molecular mass spectrometry.

Overall, this study gives an insight on the HILIC approaches that can be undertaken for separating cyclic peptides, which can be of great concern for the separation of molecules of cyclic structure, in pharmaceutical, proteomics and therapeutic applications. Furthermore, the high selectivity obtained for separating isobaric phosphopeptides might be particularly useful in proteomics to help identifying phosphorylation sites in proteins through the separation of peptides from protein digests.

Acknowledgments

The authors would like to acknowledge the CEA for its financial support.

Figure 1: Structure of the synthetic cyclodecapeptides and their positional isomers.

Figure 2: Overlay of ESIMS elution profile of each peptide in the mixture obtained in SIM mode and using mobile phase composition made of 70/30 ACN/H_2O v/v + 20 mmol L^{-1} $NH_4O_2CCH_3$. Flow rate: 300 µL min^{-1} in isocratic elution. Peptides were detected in their dicharged form $[M-2H]^{2-}$ at the following *m/z* ratios: (a) pS0 (*m/z* = 582.3). (b) pS8 and (b') pS1 (*m/z* = 601.2). (c) pS18 and (c') pS16 (*m/z* = 620.2). (d) pS168 (*m/z* = 625.7). (e) pS1368 (*m/z* = 644.6).

Figure 3: (A) ESI-MS elution profile of peptides using Acclaim HILIC-10. YMC-Triart Diol. ZIC-pHILIC and YMC-Pack SIL at different mobile phase compositions. Flow rate: 300 µL min^{-1} in isocratic elution. (a) pS0. (b) pS8 and (b') pS1. (c) pS18 and (c') pS16. (d) pS168. (e) pS1368. (B) Variation of peptide retention factors with the % of ACN in the mobile phase.

Figure 4: Variation of the retention factors *k'* according to the number of pSer residues of the peptides. The mobile phase composition was chosen to yield retention factors *k'* below 30.

References

[1] E. Mesterházy. C. Lebrun. A. Jancsó. P. Delangle. A Constrained Tetrapeptide as a Model of Cu(I) Binding Sites Involving Cu_4S_6 Clusters in Proteins. Inorg. Chem. 57 (2018) 5723–5731. https://doi.org/10.1021/acs.inorgchem.7b02735.

[2] A.M. Pujol. M. Cuillel. O. Renaudet. C. Lebrun. P. Charbonnier. D. Cassio. C. Gateau. P. Dumy. E. Mintz. P. Delangle. Hepatocyte Targeting and Intracellular Copper Chelation by a Thiol-Containing Glycocyclopeptide. J. Am. Chem. Soc. 133 (2011) 286–296. https://doi.org/10.1021/ja106206z.

[3] C. Gateau. P. Delangle. Design of intrahepatocyte copper(I) chelators as drug candidates for Wilson's disease: Intracellular copper chelation. Ann. N. Y. Acad. Sci. 1315 (2014) 30–36. https://doi.org/10.1111/nyas.12379.

[4] M. Monestier. A.M. Pujol. A. Lamboux. M. Cuillel. I. Pignot-Paintrand. D. Cassio. P. Charbonnier. K. Um. A. Harel. S. Bohic. C. Gateau. V. Balter. V. Brun. P. Delangle. E. Mintz. A liver-targeting Cu(I) chelator relocates Cu in hepatocytes and promotes Cu excretion in a murine model of Wilson's disease. Metallomics. 12 (2020) 1000–1008. https://doi.org/10.1039/D0MT00069H.

[5] M. Tegoni. F. Yu. M. Bersellini. J.E. Penner-Hahn. V.L. Pecoraro. Designing a functional type 2 copper center that has nitrite reductase activity within -helical coiled coils. Proc. Natl. Acad. Sci. 109 (2012) 21234–21239. https://doi.org/10.1073/pnas.1212893110.

[6] H. Huang. S. Chaudhary. J.D. Van Horn. Uranyl−Peptide Interactions in Carbonate Solution with DAHK and Derivatives. Inorg. Chem. 44 (2005) 813–815. https://doi.org/10.1021/ic049528l.

[7] S. Safi. G. Creff. A. Jeanson. L. Qi. C. Basset. J. Roques. P.L. Solari. E. Simoni. C. Vidaud. C. Den Auwer. Osteopontin: A Uranium Phosphorylated Binding-Site Characterization. Chem. - Eur. J. 19 (2013) 11261–11269. https://doi.org/10.1002/chem.201300989.

[8] R. Pardoux. S. Sauge-Merle. D. Lemaire. P. Delangle. L. Guilloreau. J.-M. Adriano. C. Berthomieu. Modulating Uranium Binding Affinity in Engineered Calmodulin EF-Hand Peptides: Effect of Phosphorylation. PLoS ONE. 7 (2012) e41922. https://doi.org/10.1371/journal.pone.0041922.

[9] A. Garai. P. Delangle. Recent advances in uranyl binding in proteins thanks to biomimetic peptides. J. Inorg. Biochem. 203 (2020) 110936. https://doi.org/10.1016/j.jinorgbio.2019.110936.

[10] C. Lebrun. M. Starck. V. Gathu. Y. Chenavier. P. Delangle. Engineering Short Peptide Sequences for Uranyl Binding. Chem. - Eur. J. 20 (2014) 16566–16573. https://doi.org/10.1002/chem.201404546.

[11] M. Starck. N. Sisommay. F.A. Laporte. S. Oros. C. Lebrun. P. Delangle. Preorganized Peptide Scaffolds as Mimics of Phosphorylated Proteins Binding Sites with a High Affinity for Uranyl. Inorg. Chem. 54 (2015) 11557–11562. https://doi.org/10.1021/acs.inorgchem.5b02249.

[12] M. Starck. F.A. Laporte. S. Oros. N. Sisommay. V. Gathu. P.L. Solari. G. Creff. J. Roques. C. Den Auwer. C. Lebrun. P. Delangle. Cyclic Phosphopeptides to Rationalize the Role of Phosphoamino Acids in Uranyl Binding to Biological Targets. Chem. - Eur. J. 23 (2017) 5281–5290. https://doi.org/10.1002/chem.201605481.

[13] F.A. Laporte. C. Lebrun. C. Vidaud. P. Delangle. Phosphate-Rich Biomimetic Peptides Shed Light on High-Affinity Hyperphosphorylated Uranyl Binding Sites in Phosphoproteins. Chem. – Eur. J. (2019). https://doi.org/10.1002/chem.201900646.

[14] M.L. Hennrich. V. Groenewold. G.J.P.L. Kops. A.J.R. Heck. S. Mohammed. Improving Depth in Phosphoproteomics by Using a Strong Cation Exchange-Weak Anion Exchange-Reversed Phase Multidimensional Separation Approach. Anal. Chem. 83 (2011) 7137–7143. https://doi.org/10.1021/ac2015068.

[15] A. Cristobal. F. Marino. H. Post. H.W.P. van den Toorn. S. Mohammed. A.J.R. Heck. Toward an Optimized Workflow for Middle-Down Proteomics. Anal. Chem. 89 (2017) 3318–3325. https://doi.org/10.1021/acs.analchem.6b03756.

[16] P. Hemström. K. Irgum. Hydrophilic interaction chromatography. J. Sep. Sci. 29 (2006) 1784–1821. https://doi.org/10.1002/jssc.200600199.
[17] P. Jandera. Stationary and mobile phases in hydrophilic interaction chromatography: a review. Anal. Chim. Acta. 692 (2011) 1–25. https://doi.org/10.1016/j.aca.2011.02.047.
[18] B. Buszewski. S. Noga. Hydrophilic interaction liquid chromatography (HILIC)—a powerful separation technique. Anal. Bioanal. Chem. 402 (2012) 231–247. https://doi.org/10.1007/s00216-011-5308-5.
[19] A. Periat. I.S. Krull. D. Guillarme. Applications of hydrophilic interaction chromatography to amino acids. peptides. and proteins: Liquid Chromatography. J. Sep. Sci. 38 (2015) 357–367. https://doi.org/10.1002/jssc.201400969.
[20] D.E. McNulty. R.S. Annan. Hydrophilic interaction chromatography reduces the complexity of the phosphoproteome and improves global phosphopeptide isolation and detection.. Mol. Cell. Proteomics MCP. 7 (2008) 971–980. https://doi.org/10.1074/mcp.M700543-MCP200.
[21] M. Gilar. A. Jaworski. Retention behavior of peptides in hydrophilic-interaction chromatography. J. Chromatogr. A. 1218 (2011) 8890–8896. https://doi.org/10.1016/j.chroma.2011.04.005.
[22] V. Spicer. O.V. Krokhin. Peptide retention time prediction in hydrophilic interaction liquid chromatography. Comparison of separation selectivity between bare silica and bonded stationary phases. J. Chromatogr. A. 1534 (2018) 75–84. https://doi.org/10.1016/j.chroma.2017.12.046.
[23] Y. Yang. R.I. Boysen. M.T.W. Hearn. Hydrophilic interaction chromatography coupled to electrospray mass spectrometry for the separation of peptides and protein digests. J. Chromatogr. A. 1216 (2009) 5518–5524. https://doi.org/10.1016/j.chroma.2009.05.085.
[24] S. Le Maux. A.B. Nongonierma. R.J. FitzGerald. Improved short peptide identification using HILIC–MS/MS: Retention time prediction model based on the impact of amino acid position in the peptide sequence. Food Chem. 173 (2015) 847–854. https://doi.org/10.1016/j.foodchem.2014.10.104.
[25] W. Jiang. G. Fischer. Y. Girmay. K. Irgum. Zwitterionic stationary phase with covalently bonded phosphorylcholine type polymer grafts and its applicability to separation of peptides in the hydrophilic interaction liquid chromatography mode. J. Chromatogr. A. 1127 (2006) 82–91. https://doi.org/10.1016/j.chroma.2006.05.080.
[26] S. Di Palma. P.J. Boersema. A.J.R. Heck. S. Mohammed. Zwitterionic Hydrophilic Interaction Liquid Chromatography (ZIC-HILIC and ZIC-cHILIC) Provide High Resolution Separation and Increase Sensitivity in Proteome Analysis. Anal. Chem. 83 (2011) 3440–3447. https://doi.org/10.1021/ac103312e.
[27] D. Singer. J. Kuhlmann. M. Muschket. R. Hoffmann. Separation of Multiphosphorylated Peptide Isomers by Hydrophilic Interaction Chromatography on an Aminopropyl Phase. Anal. Chem. 82 (2010) 6409–6414. https://doi.org/10.1021/ac100473k.
[28] M.J. Badgett. B. Boyes. R. Orlando. Peptide retention prediction using hydrophilic interaction liquid chromatography coupled to mass spectrometry. J. Chromatogr. A. 1537 (2018) 58–65. https://doi.org/10.1016/j.chroma.2017.12.055.
[29] P.J. Boersema. N. Divecha. A.J.R. Heck. S. Mohammed. Evaluation and Optimization of ZIC-HILIC-RP as an Alternative MudPIT Strategy. J. Proteome Res. 6 (2007) 937–946. https://doi.org/10.1021/pr060589m.
[30] M.P.Y. Lam. S.O. Siu. E. Lau. X. Mao. H.Z. Sun. P.C.N. Chiu. W.S.B. Yeung. D.M. Cox. I.K. Chu. Online coupling of reverse-phase and hydrophilic interaction liquid chromatography for protein and glycoprotein characterization. Anal. Bioanal. Chem. 398 (2010) 791–804. https://doi.org/10.1007/s00216-010-3991-2.
[31] E. Blanchard. A. Nonell. F. Chartier. A. Rincel. C. Bresson. Evaluation of superficially and fully porous particles for HILIC separation of lanthanide–polyaminocarboxylic species and simultaneous coupling to ESIMS and ICPMS. RSC Adv. 8 (2018) 24760–24772. https://doi.org/10.1039/C8RA02961J.
[32] A.J. Alpert. Electrostatic Repulsion Hydrophilic Interaction Chromatography for Isocratic Separation of Charged Solutes and Selective Isolation of Phosphopeptides. Anal. Chem. 80 (2008) 62–76. https://doi.org/10.1021/ac070997p.

494 [33] E.S. Grumbach. D.M. Diehl. U.D. Neue. The application of novel 1.7 μm ethylene bridged
495 hybrid particles for hydrophilic interaction chromatography. J. Sep. Sci. 31 (2008) 1511–1518.
496 https://doi.org/10.1002/jssc.200700673.
497 [34] https://www.ymc.co.jp/en/columns/ymc_triart_sil/. (n.d.).
498 [35] A. Yanagida. H. Murao. M. Ohnishi-Kameyama. Y. Yamakawa. A. Shoji. M. Tagashira. T.
499 Kanda. H. Shindo. Y. Shibusawa. Retention behavior of oligomeric proanthocyanidins in
500 hydrophilic interaction chromatography. J. Chromatogr. A. 1143 (2007) 153–161.
501 https://doi.org/10.1016/j.chroma.2007.01.004.
502 [36] A.J. Alpert. Hydrophilic-interaction chromatography for the separation of peptides. nucleic acids
503 and other polar compounds. J. Chromatogr. A. 499 (1990) 177–196.
504 https://doi.org/10.1016/S0021-9673(00)96972-3.
505

pS0

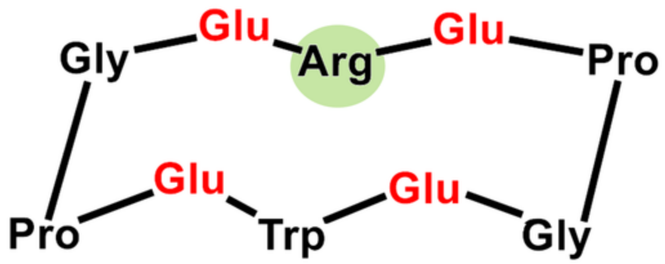

pS1

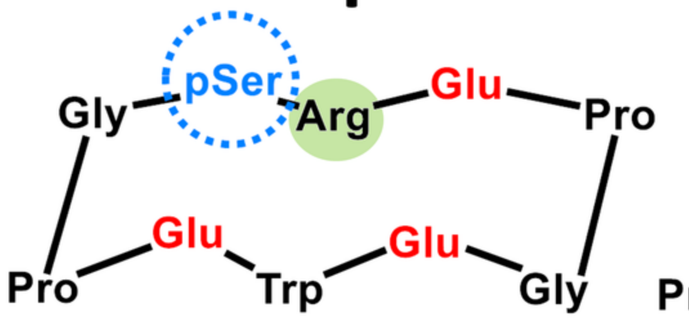

pS8

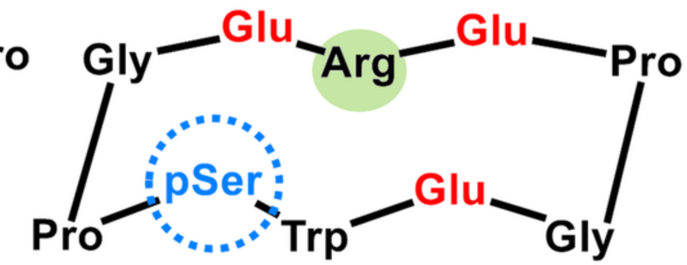

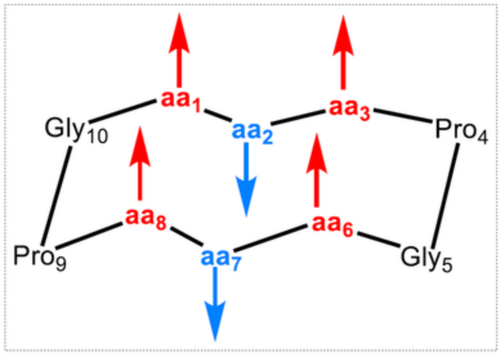

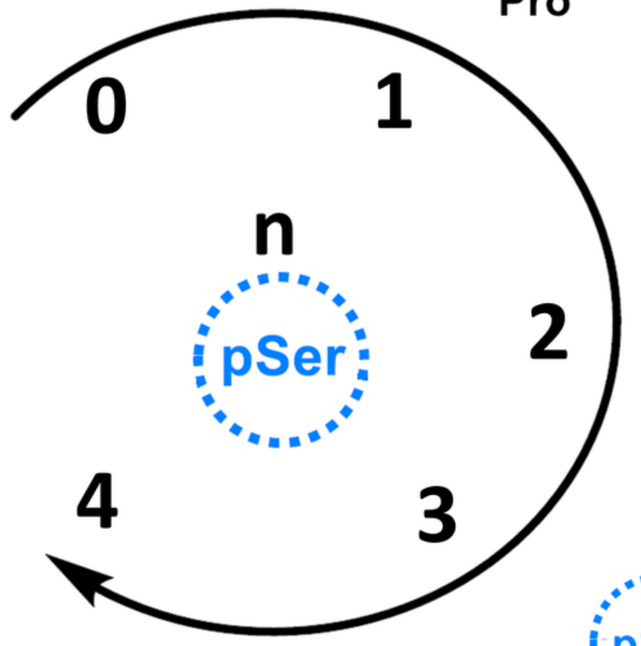

pS16

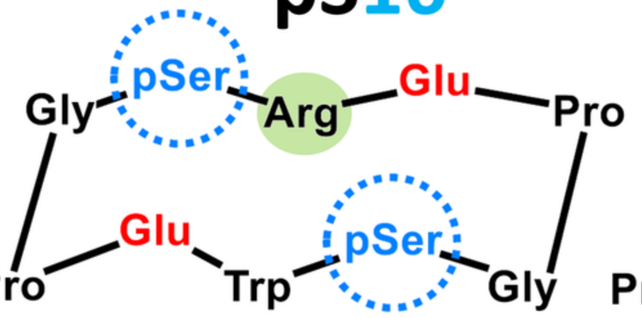

pS18

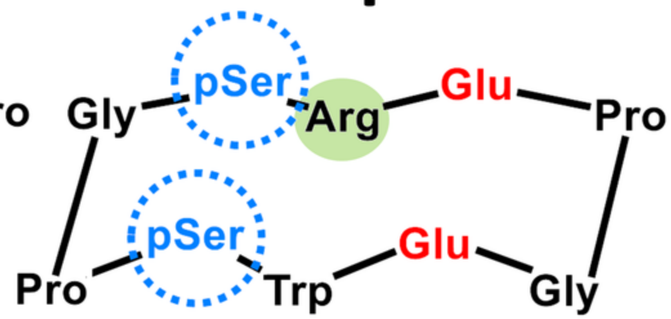

pS1368

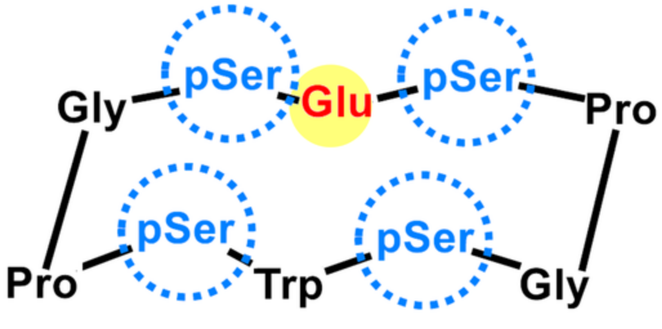

pS168

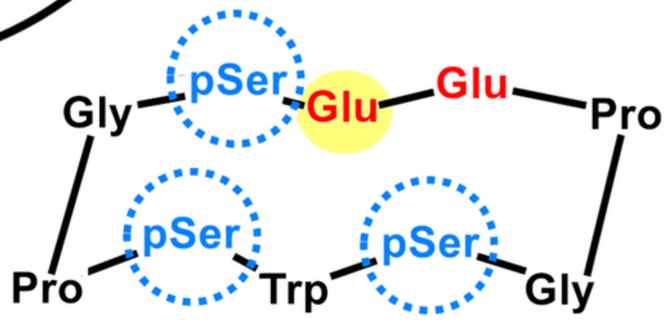

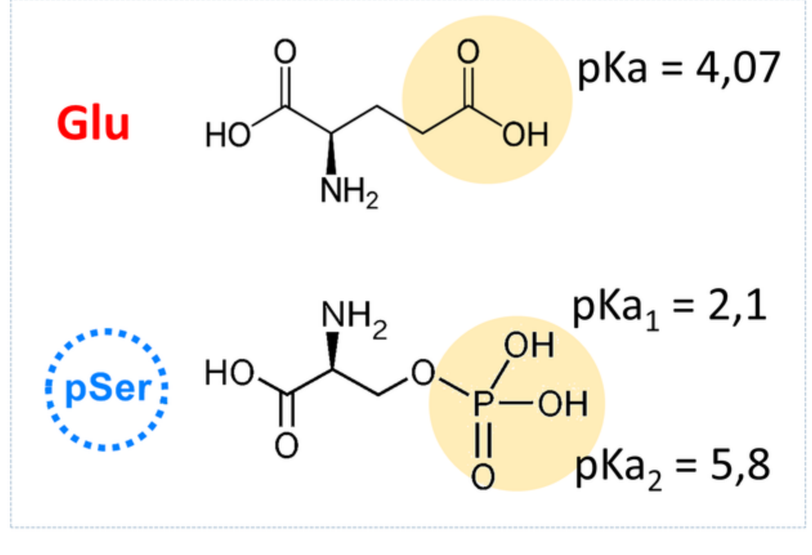

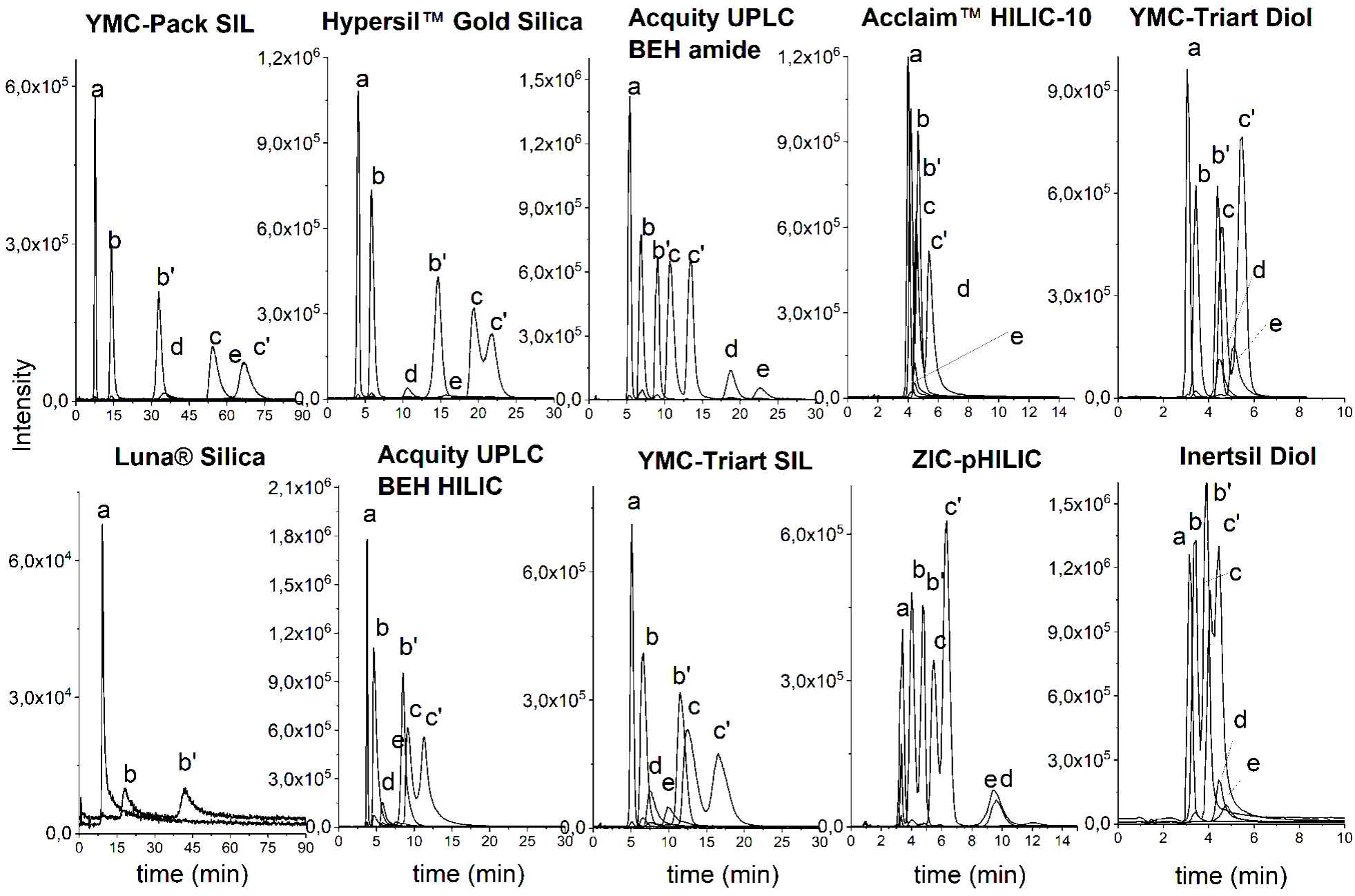
YMC-Pack SIL
Hypersil™ Gold Silica
Acquity UPLC BEH amide
Acclaim™ HILIC-10
YMC-Triart Diol
Luna® Silica
Acquity UPLC BEH HILIC
YMC-Triart SIL
ZIC-pHILIC
Inertsil Diol
Intensity
time (min)

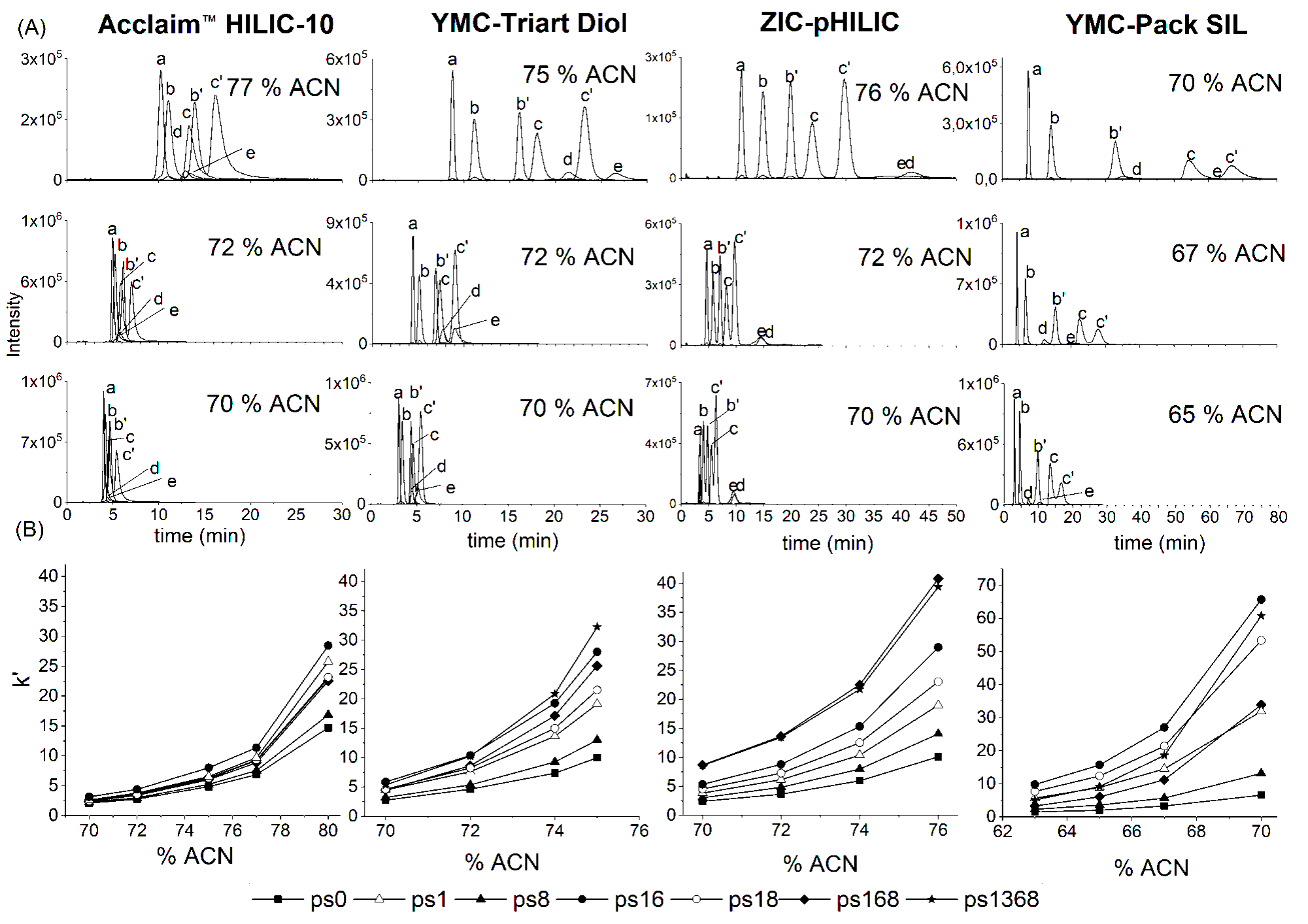
(A)
Acclaim™ HILIC-10
YMC-Triart Diol
ZIC-pHILIC
YMC-Pack SIL
77 % ACN
75 % ACN
76 % ACN
70 % ACN
72 % ACN
72 % ACN
72 % ACN
67 % ACN
70 % ACN
70 % ACN
70 % ACN
65 % ACN
Intensity
time (min)
(B)
k'
% ACN
ps0
ps1
ps8
ps16
ps18
ps168
ps1368

YMC-Pack SIL
ACN/H_2O 67/33 + 20 mM $NH_4O_2CCH_3$

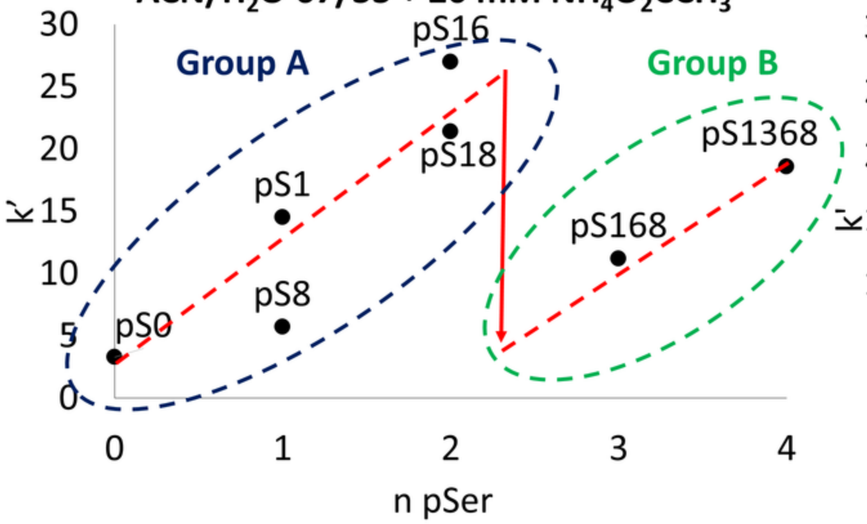

Hypersil GOLD™ silica
ACN/H_2O 70/30 + 20 mM $NH_4O_2CCH_3$

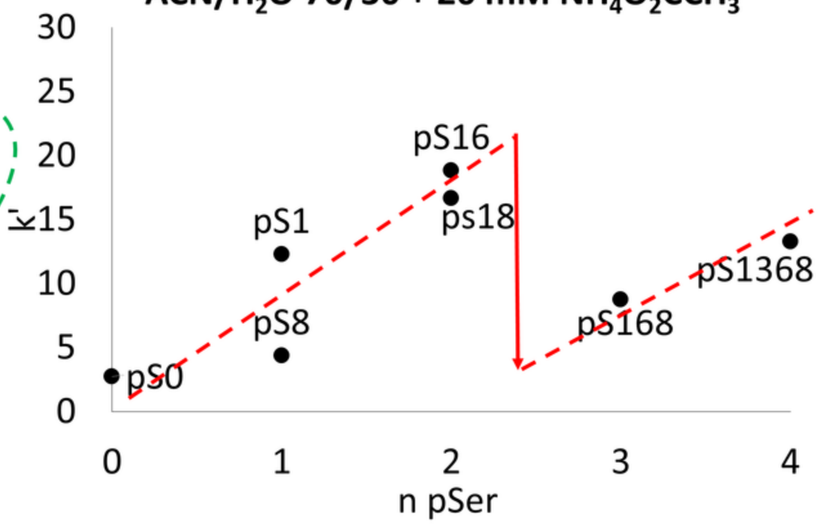

YMC-Triart SIL
ACN/H_2O 70/30 + 20 mM $NH_4O_2CCH_3$

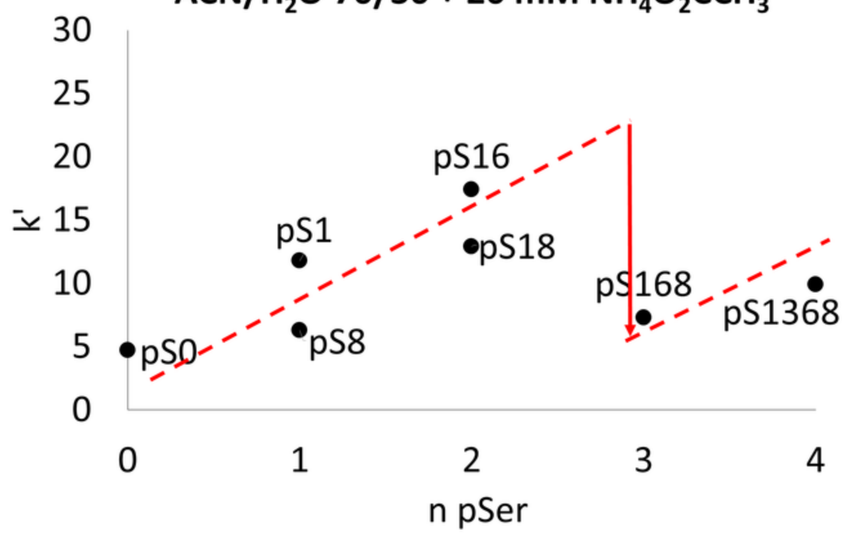

Acquity UPLC BEH HILIC
ACN/H_2O 70/30 + 20 mM $NH_4O_2CCH_3$

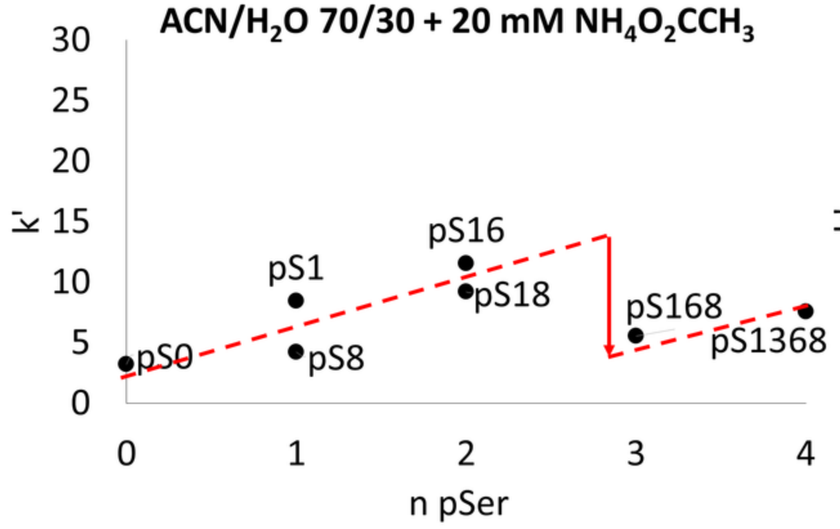

Acclaim™ HILIC-10
ACN/H_2O 77/23+ 20 mM $NH_4O_2CCH_3$

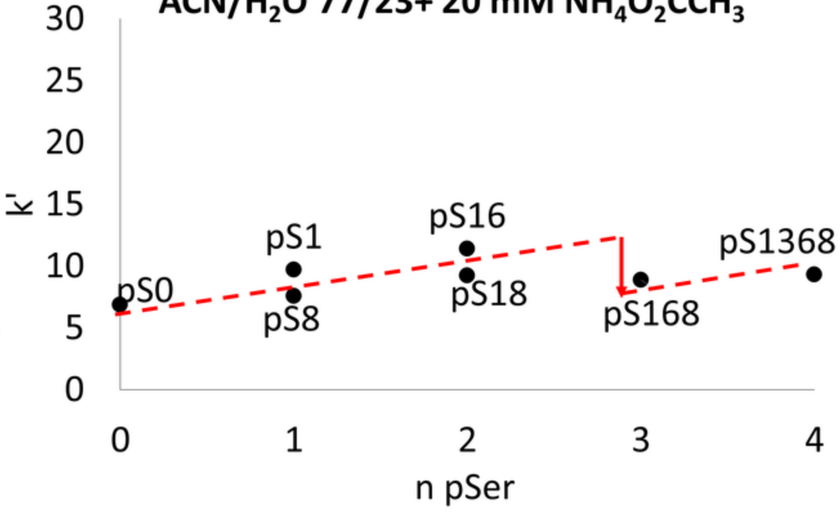

YMC-Triart Diol
ACN/H_2O 74/26 + 20 mM $NH_4O_2CCH_3$

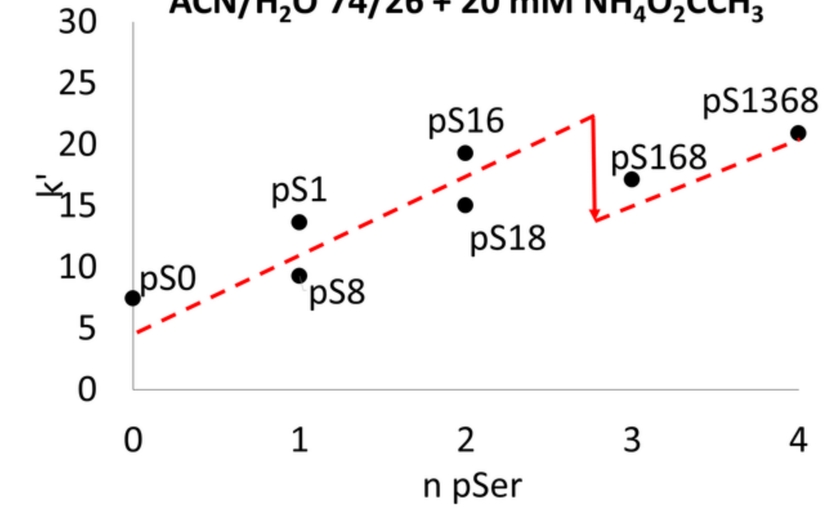

Acquity UPLC BEH amide
ACN/H_2O 70/30 + 20 mM $NH_4O_2CCH_3$

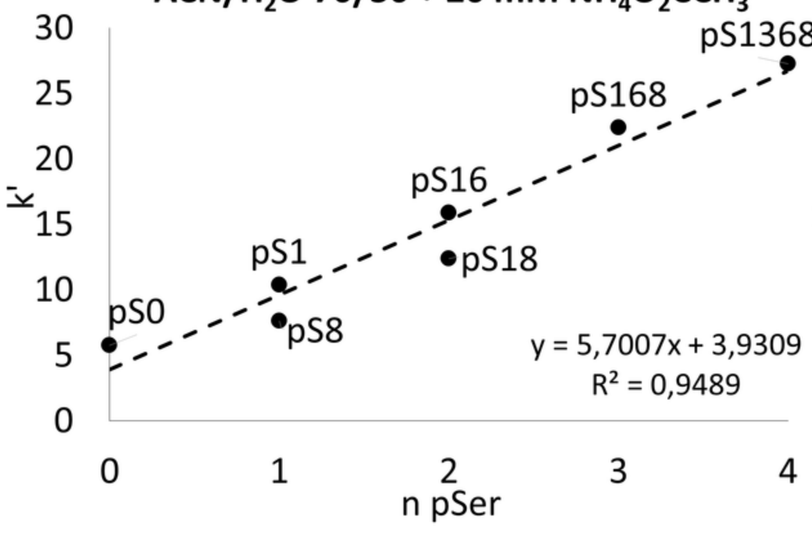

Inertsil diol
ACN/H_2O 75/25 + 20 mM $NH_4O_2CCH_3$

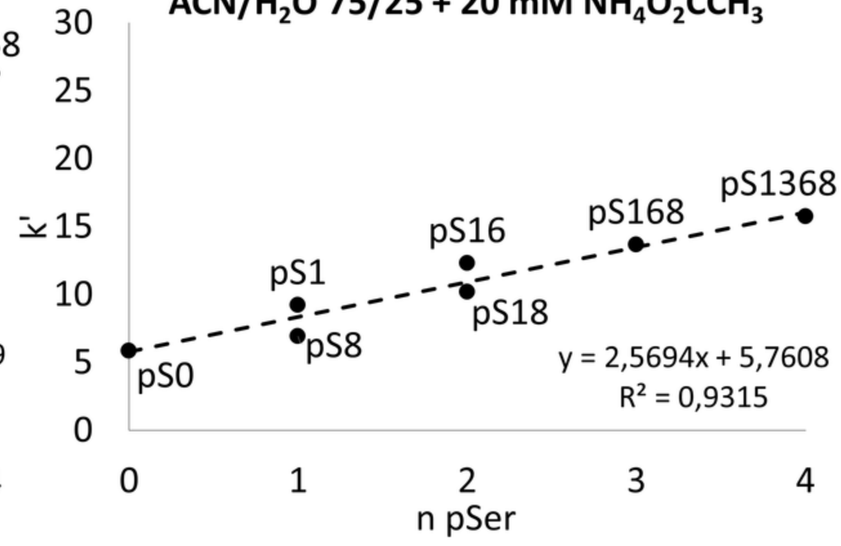

ZIC-pHILIC
ACN/H_2O 74/26 + 20 mM $NH_4O_2CCH_3$